https://rbgeomorfologia.org.br/
ISSN 2236-5664

Revista Brasileira de Geomorfologia

v. 24, nº 3 (2023)

http://dx.doi.org/10.20502/rbg.v24i3.2385

Technical Note

Low-concentrated overland flow generated in laboratory experiments: sedimentary structures and fabric

Escoamento superficial de baixa concentração gerado em experimento de laboratório: estruturas e fabrica sedimentar

Julio Cesar Paisani [1], Marcos Cesar Pereira Santos [2] e Michael Vinicius de Sordi [2]

[1] State University of Western Paraná (Universidade Estadual do Oeste do Paraná), PaleoEnvironmental Studies Center at the State University of Western Paraná (NEPA), Francisco Beltrão (PR), Brazil. E-mail: juliopaisani@hotmail.com; julio.paisani@unioeste.br
ORCID: https://orcid.org/0000-0002-8911-6477

[2] Federal University of Pelotas, Anthropology Graduate Program, Pelotas (RS), Brazil. E-mail: marcoscesar.arqueologia@gmail.com.
ORCID: https://orcid.org/0000-0003-3286-4930

[3] University of Bologna, Department of Biological, Geological, and Environmental Sciences, Bologna, Italy. E-mail: michael.sordi@gmail.com.
ORCID: https://orcid.org/0000-0001-8639-7704

Received: 29/03/2023; Accepted: 16/05/2023; Published: 26/09/2023

Abstract: The sedimentary arrangement generated by overland flows remains an open question, particularly due to the sediment concentration variations of this flow. We create a laboratory experiment to answer a question: what type of facies and structures can low concentration overland flows (≈ 3 vol%) generate in a steep-planar hillslope context with a gently sloped sand accommodation area? Our experiment revealed that nonconfined low concentrated flows were supercritical and turbulent at steep slope. On the sedimentation plain, flows exhibited progressive deceleration implying three flow stages (arrival-flow, intermediate-flow and waning-water flow). In the first stages, flows remained supercritical and turbulent, and in the last stage, they became subcritical and turbulent. Parting lineation was the predominant surface feature for the three flow stages, followed by tool marks, rills and coarse aggregate accumulation. The recurrence of flows implicated in parting lineation reworking, scour-and-fill, and horizontal airscape structures. The arrival-flow stage developed erosive depression, in which sediments were incorporated into the flow. These flow characteristics and sedimentary structures can occur in the real world and are related to overland flow recurrence.

Keywords: hillslope; overland flow; sheetwash; pedosediments; microstratigraphy; parting lineation.

Resumo: O arranjo sedimentar gerado pelos escoamentos superficiais permanece uma questão em aberto, principalmente devido às variações na concentração de sedimentos deste escoamento. Nós criamos um experimento de laboratório para responder a uma questão: que tipo de fácies e estruturas podem ser geradas pelo escoamento superficial com baixa concentração de sedimentos (≈ 3 vol%) em um contexto de encosta íngreme-plana com área de acomodação de areia levemente inclinada? Nosso experimento revelou que fluxos de baixa concentração de sedimentos são supercríticos e turbulentos. No plano de sedimentação os fluxos apresentaram desaceleração progressiva implicando três estágios de fluxo (chegada do fluxo, fluxo intermediário e fluxo de água minguante). Nos primeiros estágios, os escoamentos permaneceram supercríticos e turbulentos, e no último estágio, tornaram-se subcríticos e turbulentos. Lineações de partição foram estrutura de superfície predominante para os três estágios de fluxo, seguido por marcas lavradas por objetos, sulcos e acúmulo de agregado grossos. A recorrência de fluxos acarretou no retrabalhamento de lineações de partição, formação de estruturas de corte e

preenchimento e escape de ar horizontais. A etapa de chegada do fluxo desenvolveu depressão erosiva, na qual os sedimentos foram incorporados ao fluxo. Essas características de fluxo e estruturas sedimentares podem ocorrer no mundo real e estão relacionadas à recorrência do escoamento superficial.

Palavras-chave: encosta; escoamento superficial; pedosedimentos; microestratigrafia; lineações de partição.

1. Introduction

Hillslopes have deposits both mass wasting and overland flow (SELBY, 1994; THOMAS, 1994). Here, special attention is devoted to overland flow, considering that it is one of the main hillslope erosion agents in tropical and subtropical environments (CRUZ, 2000), primarily in sites marked by high fluvial incision, as is the case for the Volcanic Plateau of the Paraná Sedimentary Basin (VPPSB) in southern Brazil (JUSTUS et al., 1986). We conceive overland flow as synonymous with wash, rain-wash, sheet flow, and sheetwash (SELBY, 1994) and different of sheetflood. We acknowledge overland flow as a low-magnitude and high-frequency process common to a great variety of geographical contexts, whereas sheetfloods have high magnitude and low frequency, mostly in arid to semiarid areas (HOGG, 1982). Nevertheless, both processes are generated when rain intensity outperforms soil infiltration, as per Horton's (1945) conceptual terms, or when the soil becomes saturated and the water returns to the surface, although it is difficult to separate this return flow from direct precipitation (DUNNE, 1978).

Therefore, here, we conceive multiple fabric and structures that can be attributed to overland flow under varied, relatively low-magnitude and high-frequency rainfall events (BLIKRA; NEMEC, 1998; NEMEC; KAZANCI, 1999; BERTRAN; TEXIER, 1999; TEXIER; MEIRELES, 2003; MÜCHER; STEIJN; KWAAD, 2010) due to the classification gap for flow products in different scale analyses (MÜCHER, 1974; MÜCHER; MOROZOVA, 1983; MÜCHER; STEIJN; KWAAD, 2010). Such facts make it harder to identify geomorphic processes responsible for hillslope sedimentation in a wide range of continental contexts, as well as to comprehend the role of the hydraulic variables involved in generating respective deposit end-members. Hydraulic sediment erosion and transport variables by overland flow have been investigated through laboratory experiments for decades (i.e., EMMETT, 1970; MATHIER; ROY; PARE, 1989; MICHAELIDES; WAINWRIGHT, 2008; WENDLING et al., 2016; HAO et al., 2019; LIU et al., 2020) and include combining raindrop detachment-flow transport and flow detachment-flow transport systems (KINNELL, 2005). Nonetheless, fabric and structures generated by the sedimentation of overland transport material are only well documented in laboratory experiments for loessic and its reworked sediments (MÜCHER; DE PLOEY, 1977; 1984; MÜCHER; DE PLOEY; SAVAT, 1981). However, the same could not be said with regard to other materials and sediment concentrations for overland flow, as soil aggregates (pedosediments, clay balls, rounded clods, pellets, among other denominations – see Rust and Nanson (1989), Bertran and Texier (1999), Fedoroff, Courty and Guo (2010) constitute dominant fractions (ALBERTS; MOLDENHAUER; FOSTER, 1980; LIU et al., 2020) whose constituents are found on colluvial, colluvial-alluvial and alluvial microfabric and microstructures (RUST; NANSON, 1989; BERTRAN; TEXIER, 1999; BIFFI; PAISANI, 2019).

This research gap has led us to create a laboratory experiment to answer a question: what type of fabric and structures can low concentration overland flows (≈ 3 vol% of pedosediments) generate in a steep-planar hillslope context with a gently sloping sedimentation area? Such a situation is common on the transition between steep hillslopes and alluvial terraces and hollows within the VPPSB (Figure A.1 - Suppl. Mat.). We generated deposits from fluid and soil aggregates mixtures in laboratory experiments and analyzed the respective fabric and structures to improve facies taxonomy and structure analyses for overland flow colluvium in high fluvial incision hillslope contexts.

2. Materials and Methods

2.1. Experimental setup and data collections

We built a laboratory experiment simulating a planar hillslope with a slope break to create an accumulation zone (Figure 1). The slope-brake area depicts the change in morphology on the transition between hillslope bottom and valley head hollow and valley bottom lower than fourth-order stream based on Strahler's (1952) classification, here designated together as low-order valley bottoms, geomorphic units in which we have been focusing our Quaternary geomorphology studies (PAISANI et al., 2019). The experimental facility has three independent parts:

a) a mixing cylinder for water and a solid fraction to simulate overland flow; b) a wide flume (ramp) reproducing a planar hillslope; and c) a sedimentation plain to mimic low-order valley bottoms and valley hollows (Figure 1). All the experimental parts comprise an adjusted system to provide free sideways movement of the overland flow in the mixing cylinder down to the sedimentation plain.

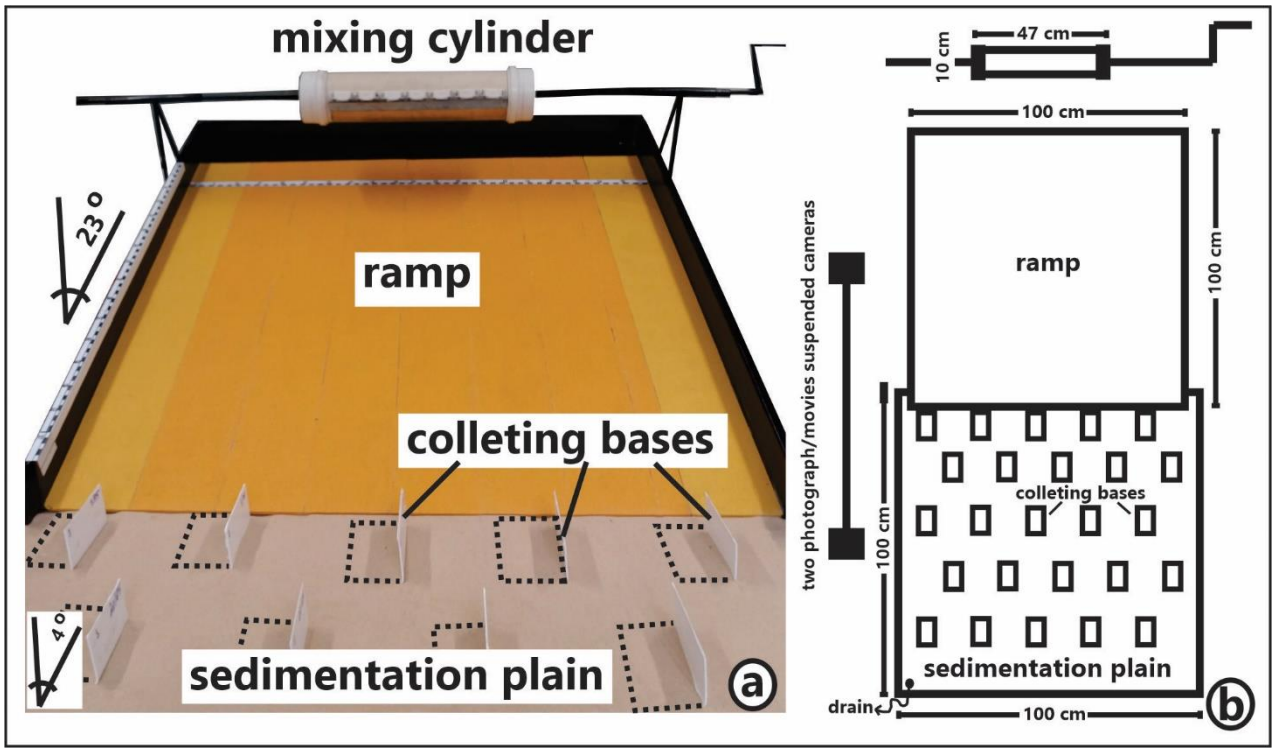

Figure 1. Laboratory experiment simulating sediment and water mixture in overland flow (mixing cylinder) fluid along a planar hillslope (ramp) and its accommodation area (sedimentation plain), which corresponds to low-order valley bottoms and valley head hollows (a). Schematic overview of the main experimental components (b).

The mixing cylinder was made from a 10 cm diameter and 47 cm long PVC tube covered on both edges (Figure 1). On one side of the cylinder, we installed an entrance/outflow port (hatch) forged in galvanized zinc with a trapdoor triggered by the weight of the mixture after the mixing cylinder stops rotating. Magnets measuring 3 x 1.7 cm were installed as immobility locks. The mixture compartment encompasses an independent mobile system that rotates on its own axis, and it is manually operated by a crank. It consists of an aerial system that maintains the granular shape of soil aggregates and was installed over two 9.5 cm high stems on the ramp's high end. The mixing cylinder had a maximum capacity (water and solid fraction mixture) of just under 3 liters.

The ramp was made from 1.8 cm thick plasticized marine plywood and has an area of 10,000 cm² (100 cm x 100 cm) and a 7 cm edge height. The inclination was set to 23°, which is equivalent to a height of 39.07 cm. To generate roughness (i.e. shear between flow and ramp), we affixed 0.80 cm grit sandpaper over the ramp floor. We kept the ramp waterproof, assuming that overland flows occur when rainfall intensity overcomes soil infiltration capacity under real-world conditions (HORTON, 1945). The ramp end had mobile and smooth contact with the sedimentation plain.

The sedimentation plain was also made from 1.8 cm thick marine plywood and had a 12,100 cm² area (110 cm x 110 cm) and a 10 cm edge height. Inclination was constant and was set to 4°. In one of the sedimentation plain bottom extremities, a drain was installed for the maintenance of the experiment. We covered the sedimentation plain bottom with a 0.5 cm thick quartz-subarcosean layer of medium to coarse sand (considering WENTWORTH, 1922 grain-size classification) as a reception bed for the sediments. Underneath the sand layer, 9 x 9 x 6 cm L-shaped collecting bases were installed to sample sediments, arranged as a rectangular regular grid. Collecting bases were made from rectangular PVC water collectors and 1 mm thick aluminium plates.

Mixture flow displacement over the ramp and the sedimentation plain were digitally registered using digital cameras placed 1.20 m above the experiment. To determine the flow displacement velocity and the real extent of sediment deposition, measuring tapes were bonded along the ramp and sedimentation plain borders. From these recordings, we calculated the flow velocity and average width, as well as the sediment accumulation morphology over the sedimentation plain. According to Ali et al. (2011), we installed groups of rulers to measure the average flux thickness (1 mm accuracy) fixed in a frame parallel to the flow direction on both the ramp and sedimentation plain.

To define flow dynamics over the ramp and sedimentation plain, we established average values of the following hydraulic parameters: sediment concentration by weight and volume, fluid density, measured flow velocity, depth of flow, cross-sectional width, area, slope, flow discharge, wetted perimeter, hydraulic radius, stream power, shear stress and Froude and Reynolds numbers (Table 1). On the occasion of flow transit over the sedimentation plain, we applied such hydraulic parameters to three stages of the flow (the arrival-flow stage, intermediate-flow stage and waning-water flow stage) to monitor respective changes. Intermediate-flow stage and water flow stage seem to correspond respectively to 'second and first hydraulic domains' in the sense of Beuselinck et al. (1999).

2.2. Fluid composition

The solid fraction is natural and corresponds to a pedostratigraphic section epipedon (code Hs13) from a rhyolitic colluvium described on the Palmas/Caçador summit surface, southern Brazil (Paisani et al. 2019). The epipedon developed approximately 0.74 ky BP. The regional modern climate is Cfa (Köppen classification), with a mean annual rainfall of 1590 $mm.y^{-1}$ that is well distributed, and an average annual temperature of 15°C (mean maximum and minimum of 26°C and 4°C, respectively). It has 6.11% organic matter; 10YR 2/1 colour of Munsell Chart; massive to subangular blocky structure; a moderately developed, silty clay loam texture (LOPES-PAISANI et al., 2016; PAISANI et al., 2019); a mixture of quartz/cristobalite, feldspar-K, pyroxene, undifferentiated iron oxides—lepidocrocite, haematite and goethite—and traces of 2:1 phyllosilicates of the smectite group (PAISANI et al., 2014), as well as a density (dry) of 2,310 kg m^{-3}.

The solid fraction of soil aggregates was generated by the maceration of subangular blocky particles later individualized by sieving fractions of mud (≤ 0.0625 mm), very fine sand, medium sand, coarse sand, very coarse sand and granules (considering WENTWORTH, 1922 grain-size classification). These fractions are formed exclusively by soil aggregates, sometimes containing primary mineral particles. We mixed these solid fractions for each repetition in equal proportions of between 6.5 and 7.5 g for each grain size.

Five consecutive flows (Run - R1 to R5) and one flow after seven days of drying of the sedimentation plain (R6) were generated. The flow fluids contained between 617 and 953.80 g of water and 46.90 to 49.80 g of sediments, resulting in an average sediment concentration of 6.08 (wt %) or 2.84 (vol %) (solid density: 2,310 kg m^{-3}). Water and sediments were mixed for around 20 s in the mixing cylinder, and agitation stopped simultaneously with the opening of the outflow hatch.

2.3. Sampling, manufacture and making of thin sections

We noticed a greater frequency of maximum longitudinal extension of the flow within the first 0.50 m of the sedimentation plain and a minor frequency between 0.70 and 1.10 m in length. Therefore, we divided the sedimentation plain into three sectors, here named proximal, median, and distal, to guide bedding microfeature sampling. Four samples were collected in the proximal sector, while for the median and distal sectors, two samples were collected for each. L-shaped collecting samplers were codified in terms of their Cartesian coordinates and horizontally oriented according to flow direction. Samples were vacuum-impregnated (15 mm Hg) with a mixture of epoxy resin, acetone and amine-based secant. The impregnated material was dried for one week in an oven at 32°C and for two more weeks outdoors for a full cure. Afterwards, the samples were cut parallel (p), or dip section, and transversely (t), or strike section, to the flow direction, and the resulting tablets were selected as representatives of sampled sectors and re-impregnated to obliterate imperfections before being bonded in glasses. Thin sections of 2.5 x 7.5 cm were then made using Metkon/GEOFORM equipment and, following the usual protocols for thin section rock, cut to an approximate thickness of 30 μm. Thin section elaboration and its respective description were carried out in the Lamination (i) and Optical Microscopy (ii) Laboratories of the Center for Paleoenvironmental

Studies (NEPA) of the State University of Western Paraná. External organization was described based on Campbell (1967), while selection was estimated by visual comparison with Harrel (1983) diagrams.

3. Results and Interpretations

3.1. Flow dynamics and sediment deposition on the ramp

On the ramp, repeated flows of water and sediment were released via free fall from the mixing cylinder. This led to the spreading of flows over the ramp, generating non-confined flows. Such behaviour divided them into smaller flows in the central water flow sheet and side branches, in which the first had its average velocity measured. The average measured velocity on the ramp was high (1.67 m s^{-1}) and gradually decreased on the sedimentation plain (0.73 to 0.22 m s^{-1}) (Table 1). The high average velocity of the flow on the ramp was higher than the previously obtained velocities in experiments with flume slope smaller than that in our experiment and erodible beds (ALI et al., 2012; GUO; CAI; WU, 2017; LIU et al., 2020), as expected. In turn, the high initial velocity of the flows reflected the expressive values of the hydraulic parameters, such as stream power, shear stress, and the Froude and Reynolds numbers (Table 1). The Froude and Reynolds numbers denoted that the ramp flows were supercritical and turbulent, indicated prevailing inertial forces against gravity (Froude) and viscosity (Reynolds). Stream power and shear stress indicate that the flow on the ramp had great transport capacity and competence (LIU et al., 2020). Nevertheless, between flow repetitions, some coarse sand (0.5 to < 1 mm)- to granule (2 to < 4 mm)-grain-sized material were deposited not only adjacent to the water flow sheet but also along the side branches with smaller flows (Figure 2). In both situations, we observed that the average flow depth was approximately three times smaller than that from the head sheet flow. Although it was not possible to determine the transport mechanism of the sediments along the experimental ramp, it is possible that the transport of the other grain sizes was by suspension/saltation and rolling (bed-load) (ASADI et al., 2007; HAO et al., 2019), as would be expected for low concentration flows of sediment (fluidic dynamic behaviour).

Table 1. Average values of hydraulic parameters for flows generated throughout the experiment in the ramp sections and sedimentation plain.

Parameter	**Ramp**	**Sedimentation plain**		
	Flow stages			
		Arrival-flow	Intermediate-flow	Waning-water
V	1.67	0.73	0.48	0.22
h	0.045	0.055	0.035	0.035
W	0.06	0.05	0.04	0.05
S	0.42	0.07	0.07	0.07
ρ	1,030	1,030	1,030	1,030
A	0.003	0.003	0.001	0.002
P	0.150	0.160	0.110	0.120
Q	0.0045	0.0020	0.0007	0.0004
R	0.018	0.017	0.013	0.015
ω	320	28	12	5
τ_o	191	39	25	25
Fr	4.0	1.8	1.4	0.6
Re	29,940	12,497	6,085	3,196

V: measured flow velocity (m s^{-1}).

h: depth of flow (m)

W: cross-sectional width (m)

S: slope (m m^{-1})

ρ: mixture density (kg m^{-3}).

A: cross-sectional area (m^2)

P: wetted perimeter (m)

Q: flow discharge (m^3 s^{-1})

R: hydraulic radius A/P (m)

ω: stream power $\rho gQS/W$ (W m^{-2}), where gravitational acceleration, g: 9.8 m s^{-2}

τ_o: shear stress -ρghS (N m^{-2})

Fr: Froude number $V/\sqrt{(g.h)}$ (-)

Re: Reynoulds number VR/v (-), where water kinematic viscosity, v (m^2 s^{-1}).

On the sedimentation plain, each flow repetition went through distinct maximum distances (0.48 to 1.1 m), although all of them had three stages of hydraulic behaviour: arrival-flow, intermediate-flow, and waning-water flow. For the arrival-flow stage, the average velocity decreased 56% (0.73 m s^{-1}) in comparison with the ramp flow velocity (1.67 m s^{-1}) (Table 1). Such a decrease in average velocity occurs due to the slope-break between the ramp (S = 0.42 m m^{-1}) and sedimentation plain (S = 0.07 m m^{-1}) (Table 1). And it was aided by a 0.5 cm level drop due to the high connection between those two parts of the experiment. Abrupt changes in the gradient fostered a direct impact on the sedimentation plain sand floor, generating an erosive depression of asymmetric concave-up morphology ≈ 0.05 m long.

On the occasion of outflow from such erosive depression, there was an increase in average depth (+22%, 0.055 m) and therefore, a reduction in hydraulic parameters of stream power, shear stress and the Froude and Reynolds numbers (Table 1), leading to partial energy dissipation of the flows similar to that observed in field investigations of natural overland flow (EMMETT, 1978). The same behaviour occurs for the intermediate-flow stage with a reduction in the average flow velocity (-34%, 0.48 m s^{-1}) and average flow height (-37%, 0.035 m) compared to the previous stage. In both cases, The Froude and Reynolds numbers show that flow remained supercritical and turbulent, with stream power and shear stress with significant transport capacity and competency. Erosive depression development undermines application of hydraulic models concept of 'area of net deposition' (HAIRSINE; BEUSELINCK; SANDER, 2002). Waning-water stage flows maintained an average high (0.035 m) but presented a lower average velocity (-54%, 0.22 m s^{-1}) and consequently, a reduction in hydraulic parameters (Table 1), resulting in a subcritical and turbulent flow regime.

A progressive decrease in flow velocity along the sedimentation plain is also related to the increase in sand bed shear, especially due to water in the bed (infiltration) after the consecutive runs (R2-5). After each flow, we noticed progressive development of the moisture lateral front until it occupied 100% of the sedimentation plain. Previous moisture conditions of the sedimentation plain were decisive to the maximum extensions of flows. Under dry bed conditions (R1, 2, 6), flows propagated for distances of 0.48 to 0.51 m (equivalent to half of the ramp length), whereas under wet bed conditions (R3-5), flows propagated down to 0.88 m and under complete saturation down to the sedimentation plain physical edge and towards the drain (which is equivalent to a greater distance than that of the ramp).

Such observations denote that, in successive repetitions, saturation conditions obliterate the infiltration effect on braking flows and favour their propagation progressively down to the experimental physical border. Such conditions are analogous to real-world hillslope hydrology, in which overland flow becomes controlled by complete soil saturation, which individualizes it as saturation overland flow (DUNNE, 1978).

3.2. Surface Structures

We observed sediment deposition between each flow that was composed of coarse-sand to granule-grain sizes along the ramp, here designated together as 'coarse aggregates' (Figure 2). Such grain sizes suffered abrasion during displacement, generating debris that adhered to sandpaper saliences that cover the ramp floor (Figure 2). In fact, a brief stereoscope observation of the aggregates showed that they suffered abrasion due to friction with the sandpaper ramp floor, leading to subtle rounding of some aggregates before deposition. The rounding of sediments by abrasion is a common phenomenon for this type of sediment and was detected by experimentation (WANG et al., 2017).

Low competent flows prompted coarse aggregate clusters (Figure 2), whereas greater flows remobilized coarse aggregates downward on sedimentation plains (Figure 3). Coarser sediments temporarily deposited on our experimental ramp resemble the transport-deposition dynamics of natural hillslope overland flow; here, part of the sediment grain sizes remain temporarily stocked on the hillslope (CROKE; HAIRSINE; FOGARTY, 1999). New rainfall events capable of generating flows with greater competence and transport capacity transfer coarser sediments down to foot slopes or low-order valley bottoms. Repetition of this process configures transit zones in hillslopes where natural overland flow is reported.

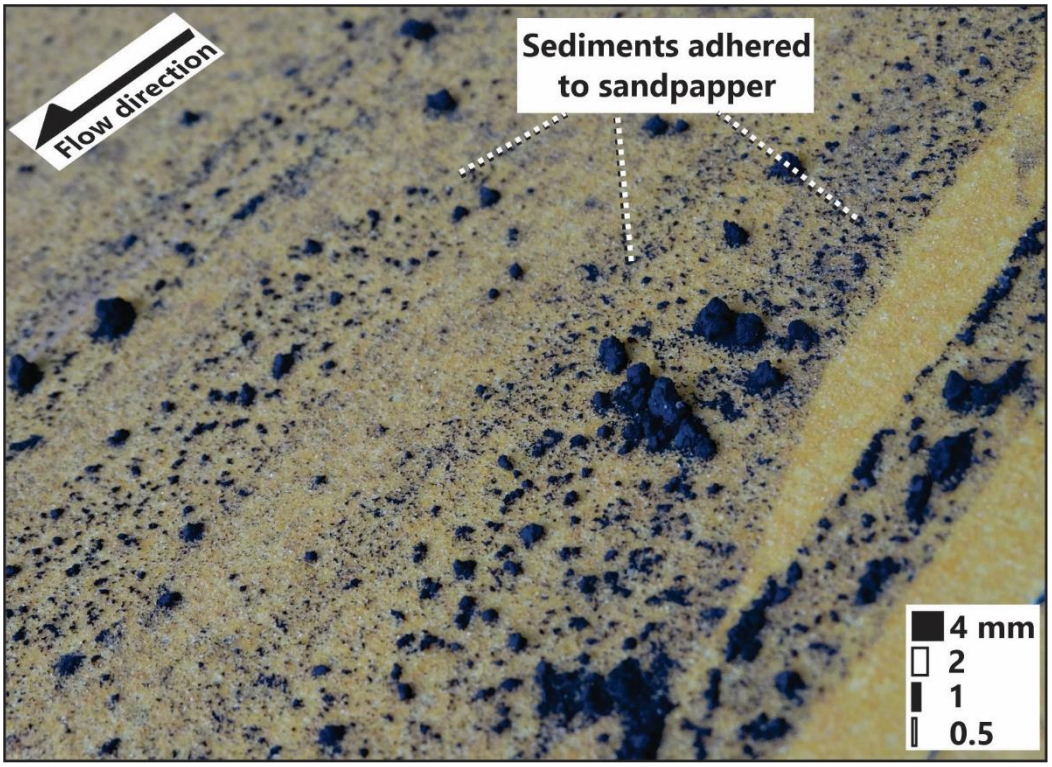

Figure 2. Coarse aggregate clusters deposited in the ramp. Picture taken between flow repetitions. It is possible to observe materials detached from the aggregates due to abrasion adhering to the sandpaper that overlaid the ramp floor.

Inside sedimentation plain the flow repetition generated coarse aggregate accumulation and scour marks. Coarse aggregate accumulation was generated on the flow head during the waning-water stage (Figure 3; Figure 4 – 25/45 laminae III, and 80/45 laminae II; Figure 5 - 10/45 laminae VI, and 15/55 laminae VI), similarly to debris flow experiments (DE HAAS et al., 2015). As for waning-water flow stage the transport capacity is not significant and is independent of inflow sediment concentration and sediment size (BEUSELINCK et al., 1999). The sediment load from this deposit type increased with coarse granules disposed on the sand bed not only after each flow repetitions but also when reworking the front limits of preceding short flows. The accumulation morphology of coarse aggregates varied between irregular tracks and tongues on smaller lateral ramifications, here named 'coarse accumulation strips' and 'coarse tongues', respectively (Figure 3; Figure 4 – 80/45).

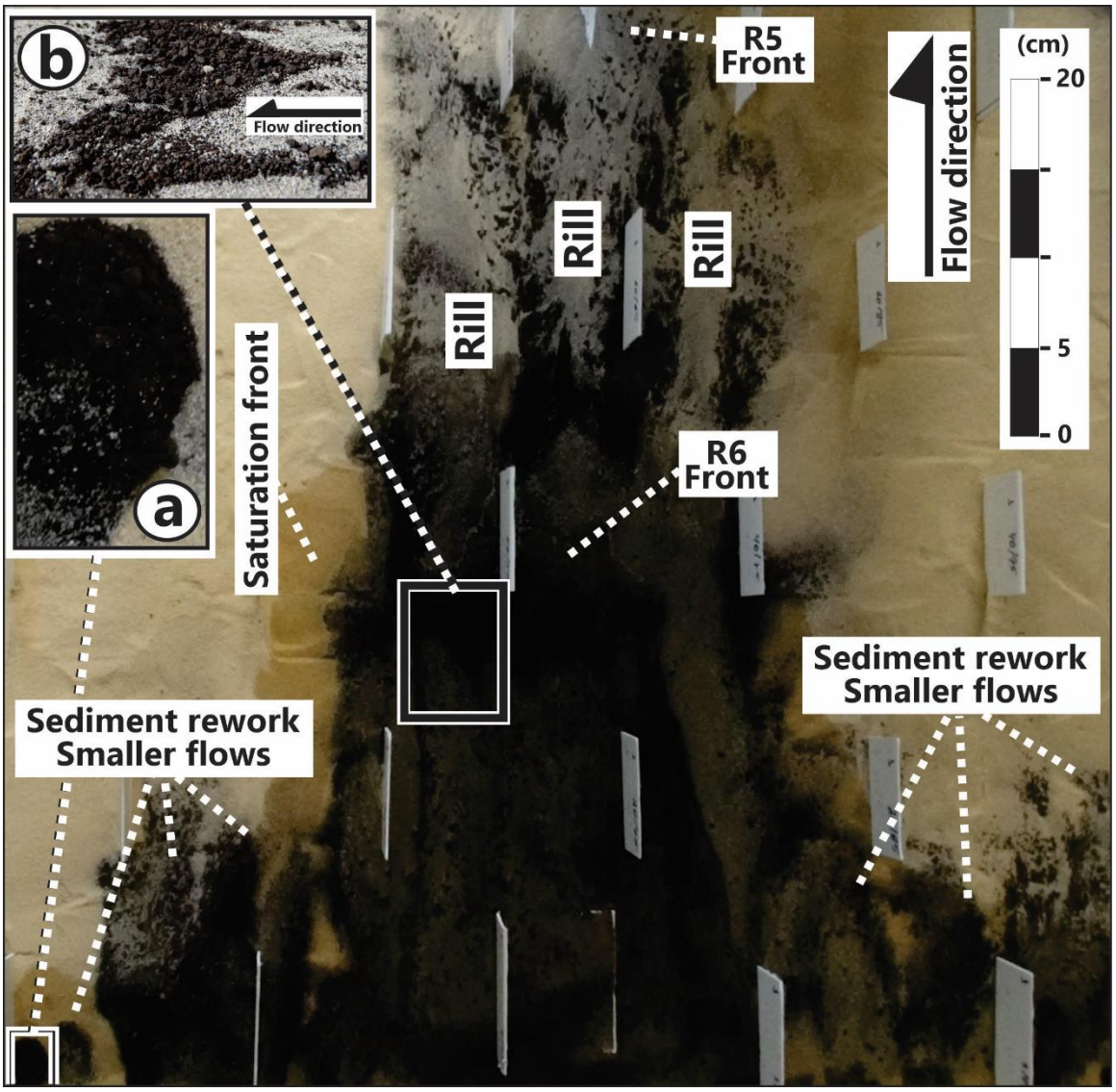

Figure 3. Surface features of the sedimentation plain. (a) Coarse tongues generated by the smaller flows of side branches. (b) Coarse *accumulation strips* generated in the frontal limit of the last flow repetition (R6).

We observed different scour and tool mark types: parting lineation, rills, obstacles and grooves (Figure 3). Parting lineation consists of low, parallel ridges and hollows with a relief seldom greater than the diameter of a few grains and is the result of supercritical flows and large bed shear stresses (ALLEN, 1984), as seen in ephemeral streams (PICARD; HIGH JR, 1973).

Parting lineation is a dominant surface feature and was preserved in the median and distal sectors of the sedimentation plain (Figure 6 – 30/45, 65/55, and 80/45). In the proximal sector, parting lineation was reworked by flow recurrence resulting in complete burial or only preserved crests (Figure 5 - 10/45, 15/55, 20/45, and 25/45).

Rills developed on the distal sector of the sedimentation plain due to flows with maximum longitudinal extension (Figure 3). They expanded to the median sector as a result of a subtle level reduction (≈ 5 mm) between the sand bed and marine plywood. Analysis of thin sections revealed that rills evolved from flow concentration on the hollows of parting lineations (Figure 3; Figure 6– 80/55, and 65/45). Obstacle marks are less frequent features and were generated from the spatial dispersion of coarse aggregates contained on coarse accumulation strips as a reflection of consecutive flow incidence (Figure 3; Figure 5 – 115/55). Groove marks of the skip and roll type are associated with coarse accumulation strips and were preserved in the distal sector due to the smaller incidence of flow repetition (Figure 4 - 80/45).

Surface features generated by natural overland flow in granular materials have received little attention. In valley head areas of the VPPSB, scattered coarse aggregates and scour marks were identified in modern colluvium

and used as interpretation keys of the Quaternary sedimentary structures (OLIVEIRA; BEHLING; PESSENDA, 2008; OLIVEIRA et al., 2008). This leads us to assume that the surface features identified in our experiment are prone to being present within deposits generated by natural overland flow in high fluvial dissected areas, as is the case for the PBVP in southern Brazil.

3.3. Bedding fabric and structure

Parallel (dip) section cuts to the flow at a macroscopic scale show that deposition produced laminae on the arrival sector of the sedimentation plain Thin sections parallel and oblique to the flow directions revealed that laminae varied from 0.25 to 2.3 mm thick with surface discontinuous wavy nonparallel, discontinuous, even parallel, continuous wavy nonparallel, continuous wavy parallel and continuous even parallel structure, herein simply designated wavy parallel, wavy nonparallel and even parallel structure, respectively, according to Campbell (1967) (Table A.1 - Suppl. Mat.). Lateral extension dominated the convergence and intersection of the bedding surface, with secondary occurrence of abutting against an unconformity and lateral gradation bedding surfaces becoming indistinguishable. All laminae presented closed packing of quartz/arcosian mixtures of sandy beds with soil aggregates and textures varying from very fine sand to granule, implying different levels of selection (very poorly sorted, poorly sorted, moderately well sorted, and well sorted). Fabric/orientation involves inverse discontinuous gradation, inverse discontinuous gradation to massive, massive, diffuse-microlaminated to massive, diffuse-cross-microlaminated (increscent angle 5–25°, 20–40°, 25–35°, 25–45°, and 30–40°) and diffuse-folded microlaminated (Table A.1 - Suppl. Mat.). We observed significant variations in these attributes and in laminae number between thin sections parallel and oblique to the flows, in addition to 2 to 10% intergranular pores from horizontal airscapes (Figs. 4, 5, 6).

Laminae can be generated in very different circumstances (ALLEN, 1984; BRIDGE, 2003; FIELDING, 2006; SUMNER; AMY; TALLING, 2008). In our experiment, they expressed an aggradational process generated by the subvertical fallout of particles and vertical accretion and degradational-aggradational processes related to scour-and-fill. Laminae passed through different levels of deformation because of horizontal airscape.

Subvertical fallout of particles was recognized by Sumner, Amy and Talling (2008) in an annular flume study and was attributed to the rapid deposition of sediments because of flow deceleration. In our experiment, they are disposed of in the sedimentation plain surface or at the aggradation layer base, sometimes embedded at subjacent levels or reworked by overlying sediments, and are common in thin sections parallel and oblique to the flow (Figure 4 - 15/45 laminae I, and IV; 40/55 laminae I; 65/55 laminae I; 80/45 laminae I; Figure 5 - 10/45 laminae III; 15/55 laminae III; 20/45 laminae I; 25/45 laminae I; Figure 6 – 40/55 laminae I; 65/55 laminae I; 80/45 laminae I). The microstructure resulting from this process is generated when flows arrive at the waning-water flow stage. At this stage the transport capacity of the flow is not significant (BEUSELINCK et al., 1999). Due to different longitudinal extensions of the flows, such microstructure is disposed from the proximal to the distal sectors of the sedimentation plain (Figures. 4, 5, 6).

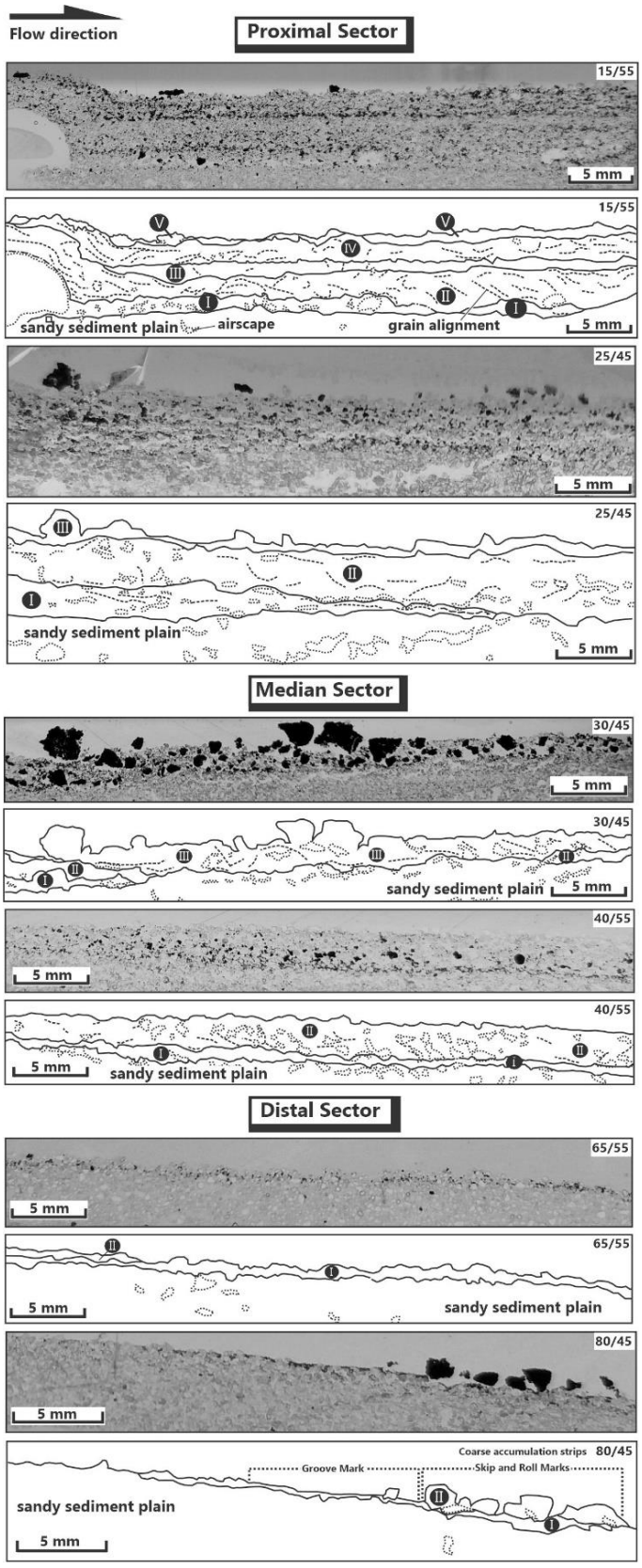

Figure 4. Photographs and sketches of laminae transverse (or strike) to flow in the proximal, median and distal sectors of the sedimentation plain. The sediments in black correspond to soil aggregates, while the sediments in white represent the quartz/arkose substrate. Polygonal incontiguous lines limit the airscape structures. Discontinuous lines indicate the banded orientation of the bigger sediment axes, while contiguous lines distinguish laminae limits. Roman numerals indicate the laminae sequence.

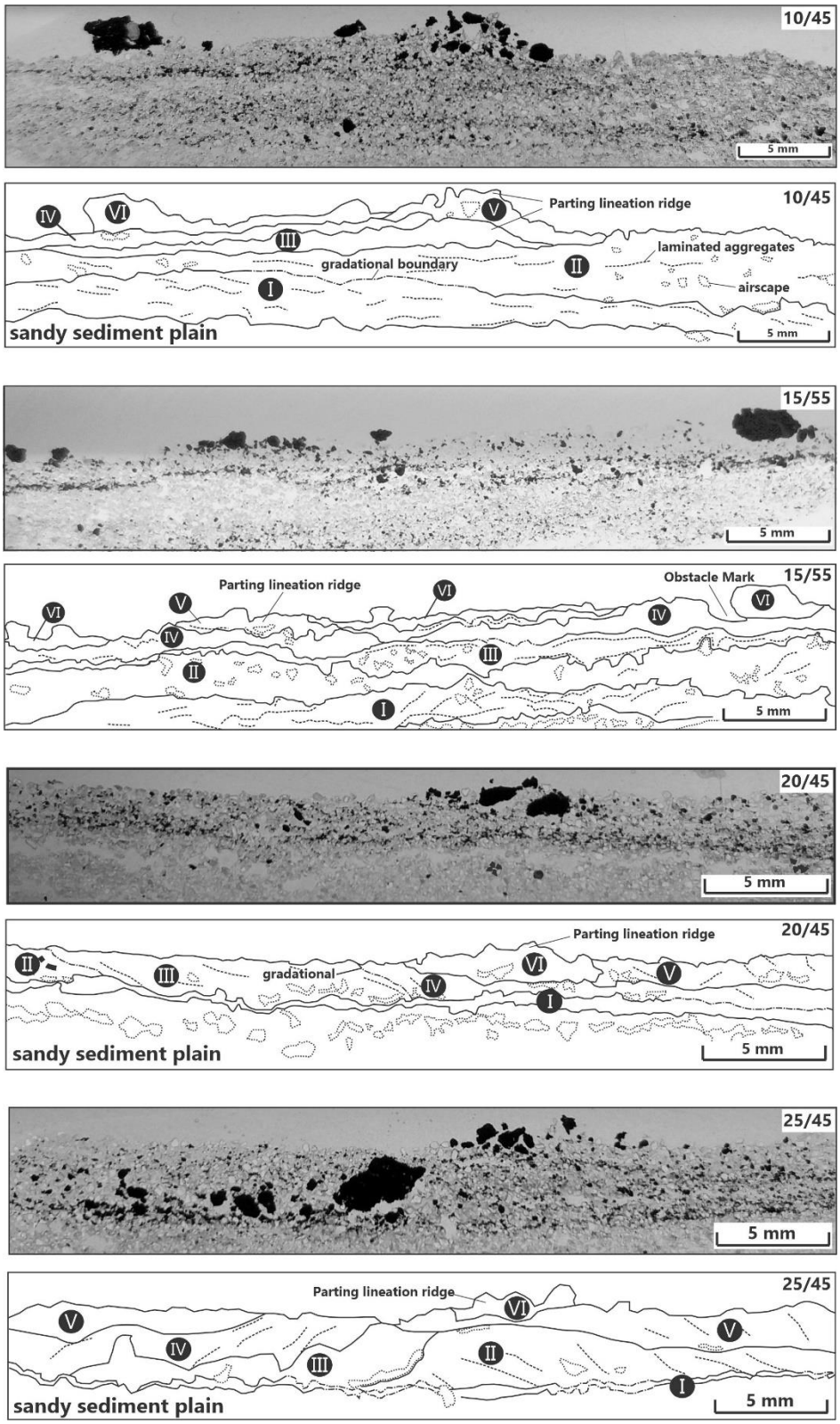

Figure 5. Photographs and sketches of laminae transverse (or strike) to flow in the proximal sector of the sedimentation plain, which had a greater incidence of flow repetitions. The sediments in black correspond to soil aggregates, while the sediments in white represent the quartz/arkose substrate. Polygonal incontiguous lines limit the airscape structures. Discontinuous lines indicate the banded orientation of the bigger sediment axes, while contiguous lines distinguish laminae limits. Roman numerals indicate the laminae sequence.

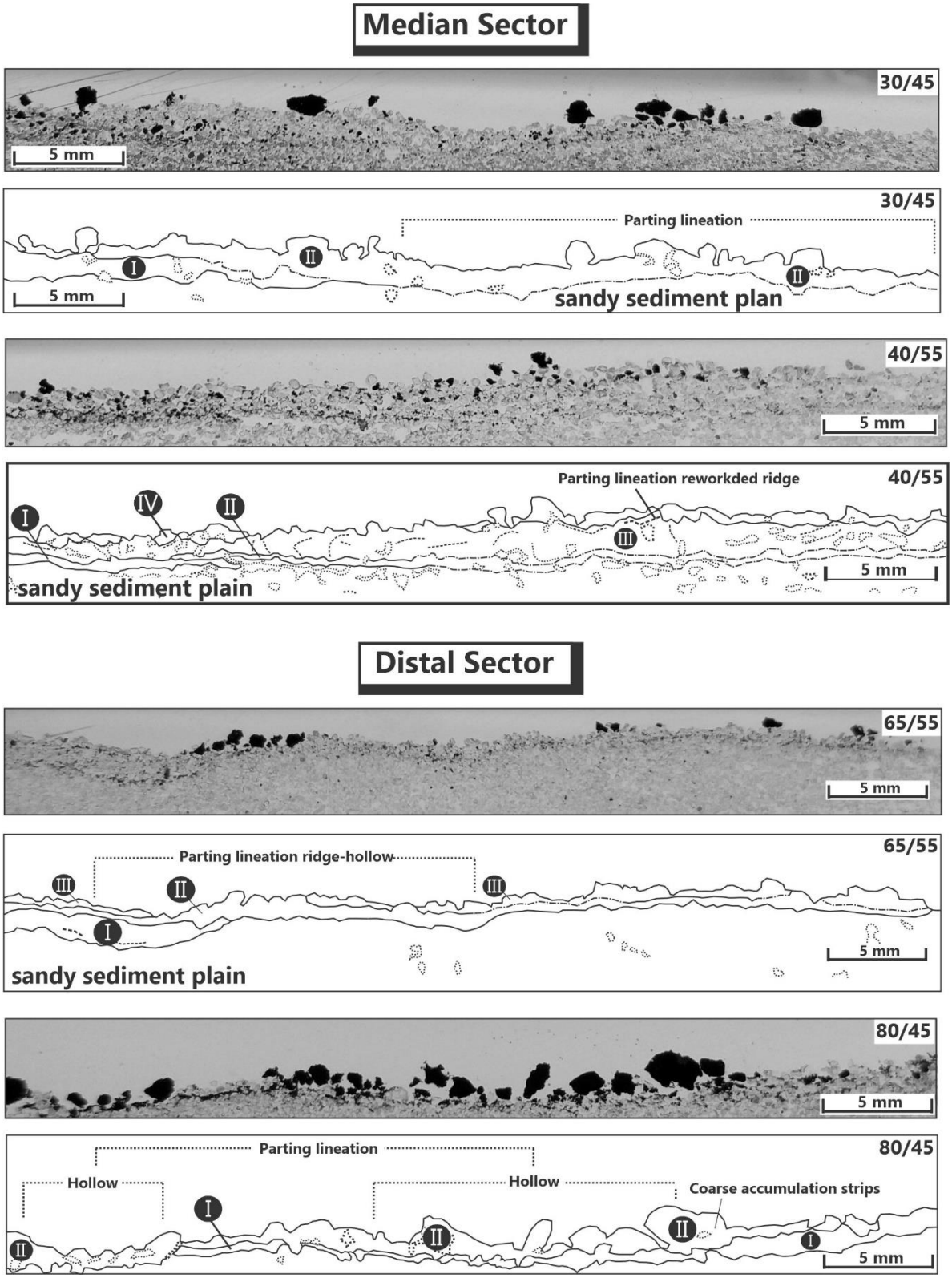

Figure 6. Photographs and sketches of laminae transverse (or strike) to flow in the median and distal sectors of the sedimentation plain. The sediments in black correspond to soil aggregates, while the sediments in white represent the quartz/arkose substrate. Polygonal incontiguous lines limit the airscape structures. Discontinuous lines indicate the banded orientation of the bigger sediment axes, while contiguous lines distinguish laminae limits. Roman numerals indicate the laminae sequence.

Vertical accretion generated recurrent microstructures on thin sections, parallel and oblique to the to the flow (Figure 4 -15/45 laminaes I, II, and III, 25/45 laminae II; 40/55 laminae II; 65/55 laminae II; Figure 5 - 10/45 laminaes I, II, and IV, 15/55 laminaes I, II, and IV; Figure 6 – 30/45 laminaes I and II, 40/55 laminaes II and III, 65/55 laminae II), where quartz/arcosian grains, well sorted and moderately well sorted, and diffuse-microlaminated to massive and massive fabric/orientation dominate (Table A.1 - Suppl. Mat.). That kind of sedimentation expresses the arrival flow-stage under the supercritical and turbulent flow regime, with stream power and shear stress with significant transport capacity and competence (Table 1). The greater concentration of quartz/arcosian sediments results from grain detachment in the proximal sedimentation plain where depressive erosion was established due to the gradient break between ramp/sedimentation plains (Figure 7). The incorporation of such constituents into the flow increased sediment concentration and therefore contributed to flow deceleration (KNELLER; BRANNEY, 1995) and possibly changed low-concentrated flows towards high-sediment-density flows. The reworking of coarse aggregates is another mechanism associated with vertical accretion formation (Figure 4 - 30/45).

Scour-and-fill was identified in the proximal sector of the sedimentation plain, exactly associated with the area of greater successive flow incidence (Figure 5 - 20/45 laminaes II, III, IV, and V; 25/45 laminaes III, IV, and V). Such a microstructure results from parting lineation hollows filled by quartz/arcosian-sediment-concentrated flows. The fill presents layers with dominance of quartz/arcosian grains, well sorted and moderately well sorted, and diffuse-cross-microlaminated (increscent angle 10–25º, 20–40º, 25–35º, 25–45º, and 30–40º) fabric/orientation (Table A.1 - Suppl. Mat.). When flow have low competency/transport capacity, coarse aggregates accumulated on hollows are buried, generating normal discontinuous gradation fabric/orientation (Table A.1 - Suppl. Mat., Figure 5 - 25/45 laminae III). Generally, the attributes are similar to those of the vertical accretion microstructure and are differentiated only by fabric/orientation. This led us to deduce that they were generated by flow conditions similar to those of the vertical accretion end-members.

Horizontal airscapes are common microstructures on the quartz/arcosian sedimentation plain and on most proximal layers (Figure 4, 5) and were responsible for diffuse-folded microlaminated fabric/orientation from some laminae (Figure 4 - 15/55, 25/45 laminaes I and II; Figure 5 - 15/55 laminae s I, II, and III). Such features denote the initial experimental conditions, when the sedimentation plain was dry and an air-filled porous quartz/arcosian substratum was present. Some bubbles promoted layer deformation, especially beyond depressive erosion, due to the hydraulic gradient change between ramp/sedimentation plains (Figure 4 - 15/55). Thus, in addition to air within the porous quartz/arcosian sedimentation plain, there was air integrated with the fluids in the overhang of the ramp/sedimentation plain transition (CARTIGNY et al., 2014). This implies that horizontal airscapes are penecontemporaneous to deformation structures.

4. Discussion

4.1 Concept of low-density flows and the correlation between fabric and structure generation through natural and artificial overland flow

Based on our results, we noticed that flows generated parting lineations and that laminae observed at the macroscopic scale express the association of aggradation and degradation/aggradation bedding features generated in different deceleration flow stages during flow into the sedimentation plain. The arrival-flow stage developed an erosive depression at the beginning of the sedimentation plain in which quartz/arcosian sand sediment was reworked and mixed with flow aggregates, generating vertical accretion. At this stage, flow recurrence promoted parting lineations, the filling of hollows in these features and sedimentation plain saturation and deformations due to horizontal airscape (Figure 7). The displacement flow stage is characterized by sedimentation plain degradation, forming parting lineation, coarse aggregate reworking and tool marks and rills. The waning-water flow stage shapes not only coarse aggregate accumulation but also tool marks in the flow front and subvertical fallout of particles of smaller particle sizes in the flow body (Figure 7).

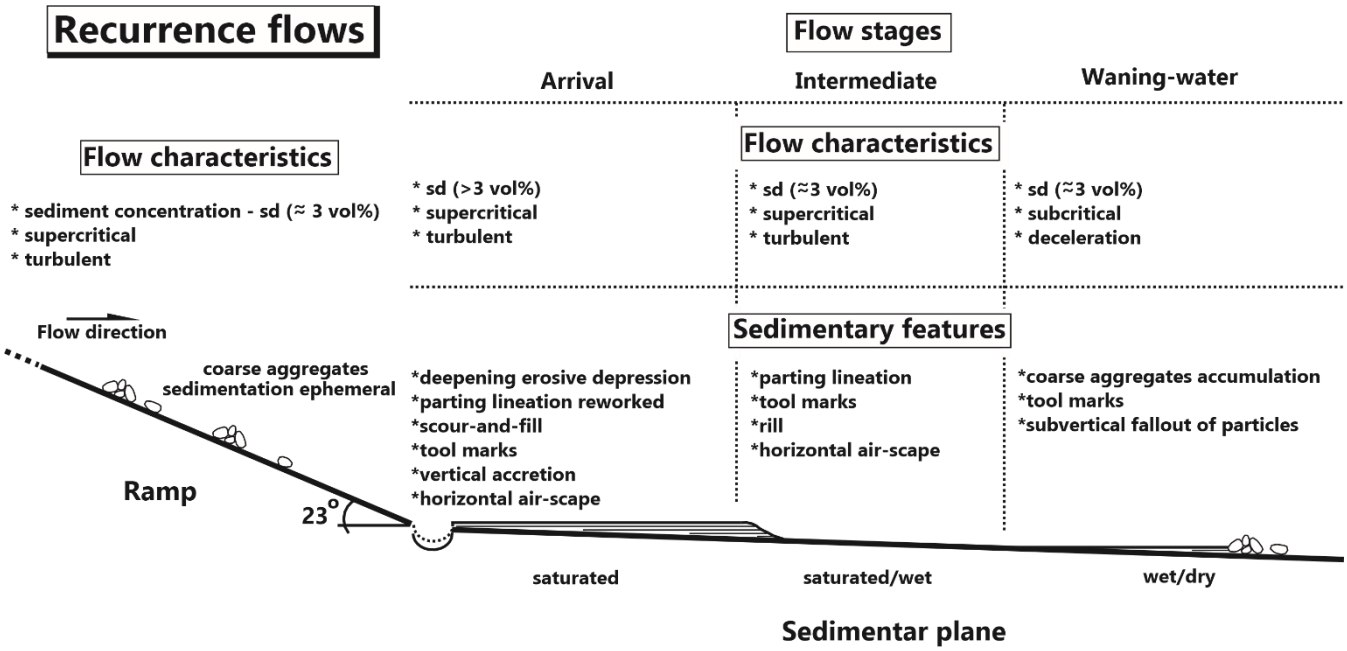

Figure 7. Characteristics of flows generated in the experiment with low sediment concentration (≈ 3 vol %) and high inclination (23°) and the features of three stage flows on the accommodation sand plain (sedimentary plain).

The perspective of rheology and fluid dynamics has contributed to the comprehension of the fabric and structure of end-members from deposits generated in subaqueous and subaerial contexts (PIERSON; COSTA, 1987; DASGUPTA, 2003; GERMAIN; OULLET, 2013). The mixture concentration (water and sediments) is one of the main parameters characterizing flow type (low-density, transitional-density, and high-density) in these perspectives (DASGUPTA, 2003). The disagreement on threshold values of low and high concentration flows between researchers is one of the main reasons for such uncertainty (SHANMUGAM, 1996). In fact, absolute values for the threshold of low-density and high-density flow types are difficult to establish because they depend on grain-size distribution, clay content, and rheological variables (PIERSON; COSTA, 1987; SHANMUGAM, 1996; MANICA, 2012). Laboratory experiments have recognized low-density turbidity currents with Newtonian flow behavior for low-volumetric concentration (< 5%) regardless of the amount of clay (MANICA, 2012). Thus, fluids generated in the present experiment correspond to low sediment concentration flows under Newtonian rheology, where gravity acts on water, and in turn affects sediment transport and deposition (BENVENUTI; MARTINI, 2002).

Descriptions of the fabrics and the deposit structures generated by overland flow are scarce. The sediment concentration in the flows responsible for the quaternary deposit fabrics and structures attributed to overland flow has not been differentiated. Flows generally indicated as 'washing' have revealed laminations with fabrics varying from random to cross (BERTRAN; TEXIER, 1999; FERREIRA; OLIVEIRA, 2006; OLIVEIRA; BEHLING; PESSENDA, 2008; OLIVEIRA et al., 2008; TEXIER; MEIRELES, 2003). In this regard, the initial conditions of the flows in our experiment were classified as low-concentration, although on the sedimentation plane there had been circumstances of sand bed reworking increasing sediment concentration, leading to the generation of end-members with massive laminae. Despite this particularity, the laminae have gradational fabric (normal to inverse) and diffuse-cross fabric while predominant. Gradational fabric (normal to inverse) represents the burial of surface structures from coarse aggregate clusters, parting lineations, rills, obstacles, and grooves, while diffuse-cross fabrics express the effects of supercritical flow on the sedimentation plane floor. The exception is in the waning-water stage where subcritical flow prevails. Similarly to that previously reported in the literature, this experiment shows that overland flow with low sediment concentration can generate laminations from very poorly sorted to well sorted, although sorting associated with a subvertical fallout of particles, vertical accretion, scour-and fill, and horizontal airscape may also occur.

5. Conclusions

This study searched for answers to the question: what type of fabric and structures can low concentration overland flows (≈ 3 vol% of pedosediments) generate in a steep-planar hillslope context with a gently sloping sedimentation area? Our experiment revealed that non-confined flow concentration is supercritical and turbulent with high values of average velocity, stream power, shear stress and Froude and Reynolds numbers, indicating significant competence/capacity of transport. On the other hand, coarse aggregates (coarse sand to granule grain sizes) sediment in different quantities along the slope between flow repetitions, whose dynamics are apparently controlled by subtle differences in the average flow depth.

On the sedimentation plain (sand accommodation area), flows had the following hydraulic and sedimentological characteristics:

i) Progressive deceleration due to topographic gradient reduction and permeability in the accommodation area, implying the generation of three flow stages (arrival-flow, intermediate-flow and waning-water- flow) and reflecting a reduction in the values of average velocity, stream power, shear stress and the Froude and Reynolds numbers. In the first stages, flows remained supercritical and turbulent, and in the last stage, flow became subcritical and turbulent.

ii) Parting lineation is the predominant surface feature for the three flow stages, followed by tool marks, rills and coarse aggregate accumulation. The latter was generated by the waning-water flow stage in association with subvertical fallout of particles. The recurrence of flows was implicated in reworked parting lineation, scour-and-fill and horizontal airscape structures.

iii) The arrival-flow stage developed an erosive depression, in which sediments were incorporated into the flow, increasing concentrations and generating quartz/arcosian sediment mixture in the sedimentation plain with soil aggregates from the flow and a vertical accretion structure.

These flow characteristics and sedimentary features had not yet been reported for depositional dynamics of overland flow but can occur in the real world, not only at the macroscopic scale, but also at the microscopic scale. In addition, they are more likely to produce an association between fabric and sedimentary structures from the three stages of the flow as a function of overland flow recurrence.

Supplementary Materials: The supplementary material for this technical note is available online at: https://github.com/revbrgeomorfologia/v24n3/blob/main/Paisani_Santos_Sordi_2023_Supplementary_Materials.pdf

Author's contributions: Julio Cesar Paisani: Writing – review and editing, writing – original draft, visualization, validation, supervision, resources, methodology, investigation, Funding acquisition, Formal analysis, Data curation, Conceptualization. Marcos Cesar Pereira Santos: Investigation, Formal analysis, Data curation. Michael Vinicius de Sordi: Writing – original draft, Formal analysis, Data curation.

Declaration of competing interest: All authors have read and agreed to the published version of the manuscript.

Financing: This reasearch was funded by the National Council for Scientific and Technological Development (Conselho Nacional de Desenvolvimento Científico e Tecnológico – CNPq) (Proc. 301039/2018-6; 302976/2021-3), the Araucaria Foundation of Paraná (Fundação Araucária do Paraná) (Conv. 021/2020 – SIT 44759; 072/2021; 288/2022), and Center for Paleoenvironmental Studies (NEPA).

Acknowledgements: Special thanks to Center for Paleoenvironmental Studies (NEPA) and to Mr. Anivaldo Lopes for the construction of the experiment.

Conflict of Interest: The authors declare no conflict of interest.

References

1. ABRAHAMS, A. D.; PARSONS, A. J.; LUK, S. H. Resistance to overland flow on desert hillslopes. **Journal of Hydrology**, n. 88, p. 343–363, 1986. DOI:10.1029/91WR01010
2. ALBERTS, E. E.; MOLDENHAUER, W. C.; FOSTER, G. R. Soil aggregates and primary particles transported in rill and interrill flow. **Soil Science Society of America Journal**, n. 44, p. 590–595, 1980. DOI:10.2136/sssaj1980.03615995004400030032x
3. ALI, M.; STERK, G.; SEEGER, M.; BOERSEMA, M.P.; PETERS, P. Effect of hydraulic parameters on sediment transport capacity in overland flow over erodible beds. **Hydrology and Earth System Sciences**, n. 16, p. 591–601, 2011. DOI:10.5194/hessd-8-6939-2011
4. ALLEN, J. R. L. 1984. **Sedimentary structures: their character and physical basis**. v.1, Amsterdam: Elsevier, 1984. 593 p.

5. ASADI, H.; GHADIRI, H.; ROSE, C. W.; YU, B.; HUSSEIN, J. An investigation of flow-driven soil erosion processes at low streampowers. **Journal of Hydrology,** n. 342, p. 134–142, 2007. DOI:10.1016/j.jhydrol.2007.05.019
6. BENNET, S. J.; ASHMORE, P.; NEUMAN, C. M. Transformative geomorphic research using laboratory experimentation. **Geomorphology**, n. 244, p. 1-8, 2015. DOI:10.1016/j.geomorph.2014.11.002
7. BENVENUTI, M.; MARTINI, I. P. 2002 Analysis of terrestrial hyperconcentrated flows and their deposits. In: MARTINI, I. P.; BAKER, V. R.; GARZÓN, G. (Eds.), **Flood and megaflood processes and deposits: recent and ancient examples**, Amsterdam: Elsevier, Spec. Publ. Int. Ass. Sediment., n. 32, p.167-193. DOI:10.1002/9781444304299.ch10
8. BERTRAN, P.; TEXIER, J. P. Facies and microfacies of slope deposits. **Catena**, n. 35, p. 99-121, 1999. DOI:10.1016/S0341-8162(98)00096-4
9. BEUSELINCK, L.; GOVERS, G.; STEEGEN, A.; QUINE, T. A. Sediment transport by overland flow over an area of net deposition. **Hydrological Processes**, n. 13, p. 2769-2782, 1999. DOI:10.1002/(SICI)1099-1085(19991215)13:17<2769::AID-HYP898>3.0.CO;2-X
10. BIFFI, V. H.; PAISANI, J. C. Micromorfologia de colúvio-alúvios em paleovoçorocas colmatadas nas superfícies de cimeira de Pinhão/Guarapuava e Palmas/Caçador – Sul do Brasil. **Revista Brasileira de Geomorfologia**, n. 20, p. 735-749, 2019. DOI:10.20502/rgb.v20i4.1642
11. BLIKRA, L. H.; NEMEC, W. Posglacial colluvium in western Norway: depositional processes, facies and palaeoclimatic record. **Sedimentology**, n. 45, p. 909-959, 1998.
12. BRIDGE, J. S. Planar and parallel lamination. In: MIDDLETON, G. V.; CHURCH, M. J.; CONIGLIO, M.; HARDIE, L. A.; LONGSTAFFE, F. J. (Eds.), **Encyclopedia of Sediments and Sedimentary Rocks**. Encyclopedia of Earth Sciences Series. Dordrecht, Boson, London: Kluwer Academic Publishers, 2003. p.534-536, DOI:10.1007/978-1-4020-3609-5_161
13. CAMPBELL, C. V. Lamina, laminaset, bed and bedset. **Sedimentology**, n. 8, p. 7-36, 1967. DOI:10.1111/j.1365-3091.1967.tb01301.x
14. CARTIGNY, M. J. B.; VENTRA, D.; POSTMA, G.; VAN DER BERG, J. H. Morphodynamics and sedimentar structures of bedforms under supercritical-flow conditions: new insights from flume experiments. **Sedimentology**, n. 61, p. 712-748, 2014. DOI:10.1111/sed.12076
15. CROKE, A. J.; HAIRSINE, P.; FOGARTY, P. Sediment transport, redistribution and storage on logged forest hillslopes in south-eastern. **Hydrological Processes**, n. 13, p. 2705-2720, 1999. DOI:10.1002/(SICI)1099-1085(19991215)13:17<2705::AID-HYP843>3.0.CO;2-Y
16. CRUZ, O. Studies on the geomorphic processes of overland flow and mass movements in the Brazilian geomorphology. **Revista Brasileira de Geociências**, n. 30, p. 504-507, 2000.
17. DASGUPTA, P. Sediment gravity flow – the conceptual problems. **Earth-Science Reviews**, n. 62, p. 265-281, 2003. DOI:10.1016/S0012-8252(02)00160-5
18. DE HAAS, T.; BRAAT, L.; LEUVEN, J. R. F. W.; LOKHORST, I. R. Effects of debris flow composition on runout, depositional mechanisms, and deposit morphology in laboratory experiments. **Journal of Geophysical Research and Earth Surface Processes ans Landformsace**, n. 120, p. 1949-1972, 2015. DOI:10.1002/2015JF003525
19. DUNNE, T. Field studies of hillslope flow processes. In: KIRKBY, M. J. (Ed.), **Hillslope hydrology**. New York: John Wiley and Sons, 1978, p. 227-293.
20. EMMETT, W. W. The hydraulics of overland flow on hillslopes. **Geological Survey Professional Paper**, n. 662-a, pp. A-66, 1970.
21. EMMETT, W. W. Overland flow. In: KIRKBY, M. J. (Ed.), **Hillslope hydrology**. New York: John Wiley and Sons, 1978. p.145-176.
22. FEDOROFF, N; COURTY, M. A.; GUO, Z. Palaeosoils and relict soils. In: STOOPS, G.; MARCELINO, V.; MEES, F. (Eds.), **Interpretation of micromorphological features of soils and regoliths**, Amsterdam: Elsevier, 2010. p.623-662. DOI:10.1016/B978-0-444-53156-8.00027-1
23. FERREIRA, G. M. S. S.; DE OLIVEIRA, M. A. T. Aplicação da micromorfologia de solos ao estudo de sedimentos alúvio-coluviais em cabeceiras de vale. **Pesquisas em Geociências**, n. 33, p. 3-18, 2006. DOI:10.22456/1807-9806.19509
24. FIELDING, C. R. Upper flow regime sheets, lenses and scour fills: extending the range of architectural elements for fluvial sediment bodies. **Sedimentar Geology**, n. 190, p. 227-240, 2006. DOI:10.1016/j.sedgeo.2006.05.009
25. GERMAIN, D.; OULLET, M. A. Subaerial sediment-water flows on hillslopes: essential research questions and classification challenges. **Progress in Physical Geography: Earth and Envorinment**, n. 37, p. 813-833, 2013. DOI:10.1177/0309133313507943
26. GUO Z, M. A. M.; CAI, C.; WU, Y. Combined effects of simulated rainfall and overland flow on sediment and solute transport in hillslope erosion. **Journal of Soils and Sediments**, n. 4, p. 1-13, 2017. DOI:10.1007/s11368-017-1868-0

27. HAIRSINE, P. B.; BEUSELINCK, L.; SANDER, G. C. Sediment transport through an area of net deposition. **Water Resources Research**, v. 38, n. 6, 1086, 2002. DOI:10.1029/2001WR000265.
28. HAO, H. X.; WANG, J. G.; GUO, Z. L.; HUA, L. Water erosion processes and dynamic changes of sediment size distribution under the combined effects of rainfall and overland flow. **Catena**, n. 173, p. 494–504, 2019. DOI:10.1016/j.catena.2018.10.029
29. HARRELL, J. A visual comparator for degree of sorting in thin and plane sections. **Journal of Sedimentary Research**, n. 54, p. 646-650, 1983. DOI:10.2110/jsr.54.646
30. HOGG, S. E. Sheetfloods, sheetwash, sheetflow, or ...?. **Earth-Science Reviews**, n. 18, p. 59-76, 1982. DOI:10.1016/0012-8252(82)90003-4
31. HORTON, R. E. Erosional development of streams and their drainage basins: hydrophysical approach to quantitative morphology. **Bulletin of the Geological Society of America**, n. 56, p. 275-370, 1945. DOI:10.1130/0016-7606(1945)56[275:EDOSAT]2.0.CO;2
32. JUSTUS, J. O.; MACHADO, M. L. A.; FRANCO, M. S. M. Geomorfologia. In: IBGE (Ed.). **Folha SH.22 Porto Alegre e parte das Folhas SH.21 Uruguaiana e SI.22 Lagoa Mirim: geologia, geomorfologia, pedologia, vegetação, uso potencial da terra**. Rio de Janeiro: IBGE, 1986. p. 313-404. Contribuição da série editada pelo extinto Projeto RADAMBRASIL.
33. KINNELL, P. I. A. Raindrop-impact-induced erosion processes and prediction: a review. **Hydrological Processes**, n. 19, p. 2815–2844, 2005. DOI:10.1002/hyp.5788
34. KNELLER, B. C.; BRANNEY, M. J. Sustained high-density turbidity currents and the deposition of thick massive sands. **Sedimentology**, n. 42, p. 607-616, 1995. DOI:10.1111/j.1365-3091.1995.tb00395.x
35. LIU, C.; LI, Z.; FU, S.; DING, L.; WU, G. Influence of soil aggregate characteristics on the sediment transport capacity of overland flow. **Geoderma**, n. 369, 114338, 2020. DOI:10.1016/j.geoderma.2020.11.4338
36. LOPES-PAISANI, S. D. L.; PAISANI, J. C.; OSTERRIETH, M. L.; PONTELLI, M. E. Significado paleoambiental de fitólitos em registro pedoestratigráfico de paleocabeceira de drenagem – superfície de Palmas-Água Doce (Sul do Brasil). **Geociências**, n.35, p. 426-442, 2016.
37. MANICA, R. Sediment gravity flow: study based on experimental simulations. In: SCHULZ, H.; LOBOSCO, R.; SIMOES, A. (Eds.), **Hydrodynamics: natural water bodies.** London: Interch Open, 2012. p.263-286. DOI:10.5772/1352
38. MATHIER, L.; ROY, A. G.; PARE, J. P. The effect of slope gradient and length on the parameters of a sediment transport equation for sheetwash. **Catena**, n. 16, p. 545-558, 1989. DOI:10.1016/0341-8162(89)90041-6
39. MICHAELIDES, K.; WAINWRIGHT, J. Internal testing of a numerical model of hillslope–channel coupling using laboratory flume experiments. **Hydrological Processes**, n. 22, p. 2274–2291, 2008. DOI:10.1002/hyp.6823
40. MÜCHER, H. J. Micromorphology of slope deposits: the necessity of a classification. In: RUTHERFORD, G. K. (Ed.), **Soil Microscopy.** Kingston, Ontario: The Limestone Press, 1974. pp. 553–566.
41. MÜCHER, H. J. ; DE PLOEY, J. Experimental and micromorphological investigation of erosion and redeposition of loess by water. **Earth Surface Processes and Landforms**, n. 2, p. 117–124, 1977. DOI:10.1002/esp.3290020204
42. MÜCHER, H. J.; DE PLOEY, J. Formation of after flow silt loam deposits and structural modification due to drying under warm conditions: an experimental and micromorphological approach. **Earth Surface Processes and Landforms**, n. 9, p. 523–531, 1984. DOI:10.1002/esp.3290090606
43. MÜCHER, H. J.; DE PLOEY, J.; SAVAT, J. Response of loess materials to simulated translocation by water: micromorphological observation. **Earth Surface Processes and Landforms**, n. 6, p. 331–336, 1981. DOI:10.1002/esp.3290060312
44. MÜCHER, H. J.; MOROZOVA, T. D. The application of soil micromorphology in Quaternary geology and geomorphology. In: BULLOCK, P.; MURPHY, C. P. (Eds**.), Soil Micromorphology**. v.1. Techniques and Applications. Berkhamsted (UK): AB Academic Publishers, 1983. p. 151–194.
45. MÜCHER, H. J.; VAN STEIJN, H.; KWAAD, F. Colluvial and Mass Wasting Deposits. In: STOOPS, G.; MARCELINO, V.; MEES, F. (Eds.), **Interpretation of Micromorphological Features of Soils and Regoliths**, Amsterdam: Elsevier, 2010. p 37–48.
46. NEMEC, W.; KAZANCI, N. Quaternary colluvium in west-central Anatolia: sedimentary facies and palaeoclimatic significance. **Sedimentology**, n. 46, p. 139-170, 1999.
47. OLIVEIRA, M. A. T.; BEHLING, H.; PESSENDA, L. C. R. Late-Pleistocene and mid-Holocene environmental changes in highland valley head areas of Santa Catarina state, Southern Brazil. **Journal South America Earth Sciences**, n. 26: 55–67, 2008. DOI:10.1016/j.jsames.2008.03.001
48. OLIVEIRA, M. A. T.; BEHLING, H.; PESSENDA, L. C. R.; LIMA, G. L. Stratigraphy of near-valley head quaternary deposits and evidence of climate-driven slope-channel processes in southern Brazilian highlands. **Catena**, n. 75, p. 77–92, 2008. DOI:10.1016/j.catena.2008.04.003

49. PAISANI, J. C.; LOPES-PAISANI, S. D. L.; LIMA, S.; RIBEIRO, F. J.; PONTELLI, M. E.; FUJITA, R. H. Paleoenvironmental dynamics of low-order paleovalleys in the Late Quaternary –Palmas/Caçador summit surface – Southern Brazil. **Catena**, n. 183, 104171, 2019. DOI:10.1016/j.catena.2019.104171
50. PAISANI, J. C.; PONTELLI, M. E.; OSTERRIETH, M. L.; LOPES-PAISANI, S. D.; FACHIN, A.; GUERRA, S.; OLIVEIRA, L. Paleosols in low-order streams and valley heads in the Araucaria Plateau – record of continental environmental conditions in Southern Brazil at the end of MIS 3. **Journal South America Earth Sciences**, n. 54, p. 57-70, 2014. DOI:10.1016/j.jsames.2014.04.005
51. PICARD, M. D; HIGH JR, L. R. **Sedimentary structures of ephemeral streams**. Developments in sedimentology 17, Amsterdam: Elsevier, 1973. 223 p.
52. PIERSON, T. C. Hyperconcentrated flow – transitional process between water flow and debris flow. In: JAKOB, M. M.; HUNGR, O. (Eds.), **Debris-flow hazards and related phenomena**. Berlin: Springer, 2005. p.159-202. DOI :10.1007/3-540-27129-5_8
53. PIERSON, T. C.; COSTA, J. E. A rheologic classification of subaerial sediment-water flows. **Geological Society of America Review and Engineering Geology,** n. VII, p. 1-12, 1987. DOI:10.1130/REG7-p
54. RUST, B. R.; NANSON, G. C. Bedload transport of mud as pedogenic aggregates in modern and ancient rivers. **Sedimentology**, n. 36: 291-306, 1989.
55. SHANMUGAM, G. High-density turbidity currents: are they sandy debris flow? **Journal of Sedimentary Research**, n. 66, p. 2-10, 1996. DOI :10.1306/D426828E-2B26-11D7-8648000102C1865D
56. SELBY, M. J. Hillslope sediment transport and deposition. In: PYE, K. (Ed.), **Sediment transport and depositional processes**, Oxford: Blackwell Scientific Publications, 1994. p. 61–87.
57. STRAHLER A. 1952. Hypsometric (area-altitude) analysis of erosional topography. **Bulletin of the Geological Society of America**, n. 63, p. 1117-1142. DOI:10.1130/0016-7606(1952)63[1117:HAAOET]2.0.CO;2
58. SUMNER, E. J.; AMY, L. A.; TALLING, P. J. Deposit structure and processes of sand deposition from decelerating sediment suspensions. **Journal of Sedimentary Research**, n. 78: 529–547, 2008. DOI:10.2110/jsr.2008.062
59. TEXIER, J. P.; MEIRELES, J. Relict mountain slope deposits of northern Portugal: facies, sedimentogenesis and environmental implications. **Journal of Quaternary Science**, n. 18, p. 133-150, 2003. DOI:10.1002/jqs.752
60. THOMAS, M. **Geomorphology in the tropics: a study of weathering and denudation in low latitudes**. Hoboken: Wiley, 1994. 460 p.
61. VAN DER MEER, J. J. M.; MENZIES, J. The micromorphology of unconsolidated sediments. **Sedimentary Geology**, n. 238, p. 213–232, 2011. DOI:10.1016/j.sedgeo.2011.04.013
62. WANG, J. G.; YU, B.; YANG, W.; CHENG, J. N.; SONG, Y. R.; CAI, C. F. The abrasion of soil aggregate under different artificial rough beds in overland flow. **Catena**, n. 155, p. 183-190, 2017. DOI:10.1016/j.catena.2017.03.016
63. WENDLING, V.; LEGOUT, C.; GRATIOT, N.; MICHALLET, H.; GRANGEON, T. Dynamics of soil aggregate size in turbulent flow: respective effect of soil type and suspended concentration. **Catena**, n. 141, p. 66–72, 2016. DOI:10.1016/j.catena.2016.02.015
64. WENTWORTH CK. 1922. A scale of grade and class terms for clastic sediments. **Journal of Geology**, n. 30, p. 377-392.